Dual Stage Actuators for High Density Rotating Memory Devices

W. Guo, S. Weerasooriya, T.B. Goh, Q.H. Li, C. Bi, K.T. Chang, T.S. Low

Data Storage Institute, 10 Kent Ridge Crescent, Singapore 119260

Abstract – **Maintaining the trend towards higher track densities and data rates in rotating memory devices require track following servo systems of increasing bandwidth for reliable storage and retrieval (R/W) of data. The bandwidth requirements are even more severe in the emerging portable computing applications. Increase in bandwidth under strict constraints on over-sampling is limited by the presence of mechanical resonance modes and other nonlinearities in the voice coil motor (VCM) actuators. One approach to overcoming the problem is by using a dual or a compound actuator. In such a mechanism, a VCM is used as a primary stage while the recording head is mounted on the secondary stage which in turn is mounted on the VCM. The secondary stage provides rapid small-motion and position correction to the recording head. Several dual-stage configurations have been proposed using electrostatic, piezoelectric and electromagnetic secondary actuators. The paper proposes a piezoelectric stack micro-actuator design for a disk drive. It preserves the present suspension and head assembly. A prototype of the actuator is designed, fabricated, and tested. The test results are presented. A dual actuator tracking servo system is proposed. The scheme is a promising alternative for providing high bandwidth actuation for future high performance drives.**

I. INTRODCUTION

A well known trend in magnetic data storage is the 60% areal density growth per annum. At this rate, an advanced magnetic storage device is expected to have around 25,000 tracks per inch. (TPI) by the year 2000. The maximum tolerable offset between the R/W head and the track center is less than 10% of the track pitch for accurate reading and writing of data. It is estimated that a drive spinning at 7500 rpm supporting the above track density would require a servo bandwidth of 2 - 2.5 kHz to accomplish the above [3].

Fig. 1 shows the Bode magnitude plot of a typical VCM actuator transfer function. Note that the transfer function has a resonance mode around 10 Hz, which is due to the presence of pivot friction. Friction causes a loss of low frequency gain of the actuator servo loop, which causes problems in settling [4]. The transfer function also displays resonant behavior at around 4 kHz, which corresponds to the quasi-rigid body mode of the actuator, which is primarily dependent on the

stiffness of the pivot bearing. Assuming that the actuator servo loop is of the form shown in Fig. 2 with a PI + Lead compensator, the resonance mode causes the open loop servo bandwidth to be limited to ≈ 400 Hz. Additional bandwidth will causes a loss in stability and high frequency rejection.
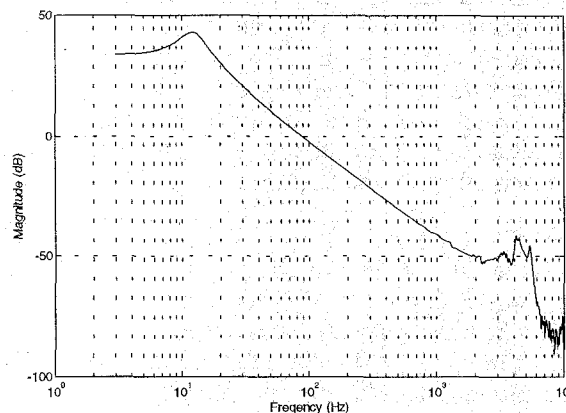
Fig. 1. Transfer function of a typical 3.5" disk drive VCM actuator.

One method that can eliminate the small signal friction and provide higher bandwidth actuation is by using a micro-actuator as a secondary stage. It can be designed to ride on the primary actuator and provide rapid small signal motion to the R/W head. Optical disk drives already use such a dual actuator arrangement very effectively in achieving >15,000 TPI track densities. Thus it is clear that a micro-actuator with a high servo bandwidth will increase the achievable track density in magnetic storage devices as well.
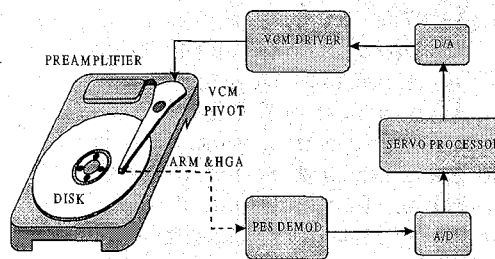
Fig. 2. Servo control system block diagram of hard disk drives.

The micro-actuator has to be small in size but yet be able to provide sufficient displacement with reasonably low control input. Many alternate designs of secondary actuators for disk drives have been reported in the literature. They include: milli-actuators driven by electromagnetic forces [4]; electrostatic forces [2]; and piezo-electric effect [3-4]. The paper reviews some of these reported designs and proposes a new stacked piezo-electric secondary actuator. The actuator is

fabricated and tested for its frequency response. A tracking servo scheme for a VCM + piezo based compound actuator is designed and simulated. Note that the words micro-actuator, dual actuator and compound actuator have been used interchangeably in the text of this paper.

II. DESIGN REVIEW OF EXISTING SECONDARY STAGE ACTUATORS

A dual stage positioning system as shown in Fig. 3 was developed by Hitachi in 1993 [1,6]. Built on a primary stage VCM, a secondary piezoelectric stack (multilayer) actuator using PZT is installed on a head-supporting arm. A pair of parallel plate springs restrains and guides the displacement of the piezoelectric element, which can precisely locate and maintain the head to a predetermined position on disk surface. The piezoelectric actuator has a stroke length of 3-4 tracks for an applied voltage of 0 to 100volts. FEM analysis results show that the resonant frequency in the positioning direction is about 7.4KHz.
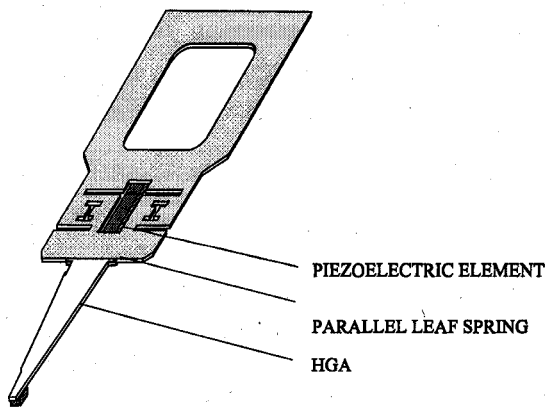
Fig.3. Piezoelectric stack actuator as secondary stage actuator.
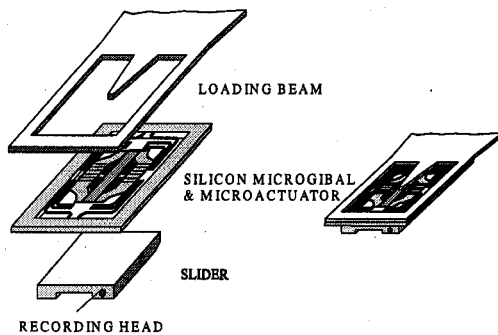
Fig. 4. Micro-gimbal electromagnetic micro-actuator.

An electromagnetic micro-gimbal secondary actuator was designed and fabricated with micro-machining techniques [2,7]. As shown in Fig. 4, the actuator consists of outside frame, planer micro-springs, coils, and a movable platform. Instead of a solid coupon in the center, the slider is attached to the micro-gimbal by a set of thin planer springs, which are designed to have maximum in-plane compliance while maintaining adequate out-of-plane pitch and roll stiffness. A

pair of thin-film variable-reluctance micro-actuators is used to move the slider in the in-plane direction, each of which consists of two pieces. The stationary piece is mounted on the outside frame and is constructed of one layer of Perm-alloy with a wrapped-around helical flat copper coil. The moving piece is attached to the slider. When a voltage is applied to the coil, magnetic force is exerted on the moving core, pulling it towards the stator resulting in an in-plane/cross-track micron-level fine motion of the slider. The design has the important advantage that the required fabrication technology is very similar to that used in making thin film heads.
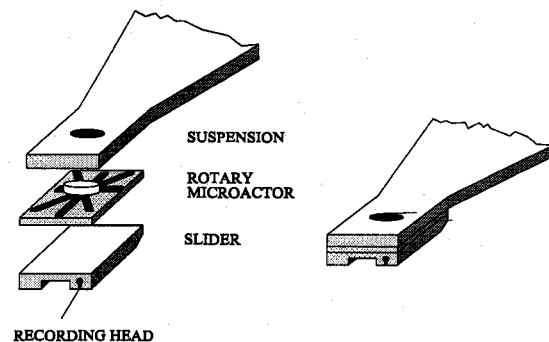
Fig. 5. Rotary electrostatic micro-actuator

Shock loads applied in the direction of in-plane motion lead to extra uncontrolled displacement of an actuator with low in plane stiffness. During high G-shock, such a displacement may be sufficient to affect the R/W process. A rotary electrostatic micro-actuator proposed by IBM [3,8], can greatly reduce such shock sensitivity and assure greater reliablility of the R/W process. As shown in Fig. 5, the micro-actuator consists of a rotating plate supported on a substrate by four linear springs. There are two sets of radial mating interdigitated electrodes on both the movable plate and substrate, which activate the motion of the plate in its tangential direction. The springs are designed to provide a sufficiently low rotational spring constant to allow rapid in-plane rotation but sufficiently high loading capability to accommodate shock loads and stiction loads. The actuator was fabricated using micro-machining techniques. The desired displacement output is about ±2 μm.
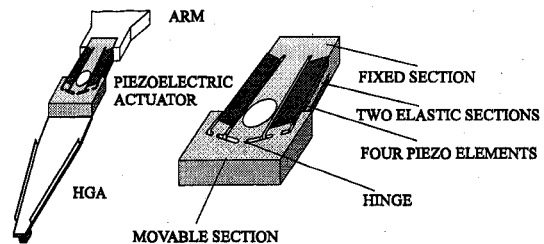
Fig. 6. Planer piezoelectric micro-actuator

Fig. 6 shows another piezoelectric micro-actuator design configuration [4]. The micro-actuators are built into the stainless head-mounting block and placed between the head-gimbal assembly (HGA) and the arm. The micro-actuator is small and light. It has four piezoelectric elements. The close-

up view illustrates that the actuator consists of three sections seperated by slits, elastic which are a movable section attached to the HGA and two elastic sections sandwiched by piezoelectric elements. Two piezoelectric elements are connected to both sides of an elastic section. When the same voltage is applied to the pairs, one expands and the other contracts longitudinally. A movable section connects to the HGA and is swung by the two pairs of the piezoelectric elements. The generated displacement is amplified eight times at the head. The application of ±12 v results in a 2-3 μm displacement. The first resonant frequency was measured to be about 3 kHz.

Yet another electromagnetic flexural milli-actuator consists of a head mounting block for the movable part, a stator magnet and a yoke on the carriage arm, a flat coil on the movable part and across-shaped spring that supports the movable part [5]. The HGA attached to the head mounting block is driven in the in-plane rotary direction around a stator shaft by electromagnetic force. The existing HGA technology can be directly employed. From experiments, the first resonant frequency is 170 Hz and the second is 9.7 kHz. A dual stage servo system has been built with 30 kHz sample frequency and 3.3 kHz servo bandwidth was achieved. It is claimed that this dual stage system can achieve servo performance required for 25 kTPI recording.

III. STACK PIEZOELECTRIC ACTUATOR WITH CROSS-SPRING
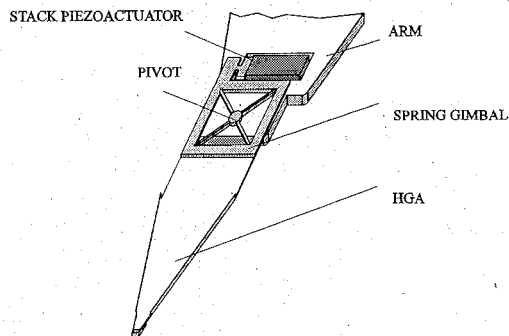
Fig. 7. Stack piezoelectric micro-actuator with cross-spring.

A simply cross structured piezoelectric micro-actuator has been designed and fabricated, as shown in Fig. 7. The piezoelectric micro-actuator is constructed with a PZT piezoelectric stack element and a cross-shaped rotational spring frame. The piezoelectric stack element is mounted on the arm. One end of the piezoelectric element is attached to the arm while the other is connected to the cross-spring frame. The cross-spring frame has a small pivot at its crossing point, which is fixed to the base of the arm. The narrow neck is used to prevent the piezoelectric element from a high bending moment. A HGA is directly connected to the edge of the cross-spring frame. It is important to note that certain preload should be applied to the cross-spring frame. When a electric voltage is applied to the piezoelectric stack element, the piezoelectric element expands or contracts, depending on the polarity of the applied voltage. This activates the rotation

of the cross-shaped spring frame around its pivot leading to the amplification of the displacement output at the recording head. The present HGA can be directly used without any modification, and thus the dynamics of the HGA will remain unchanged.

The cross-spring frame is the most critical component of the secondary piezoelectric micro-actuator. Its structure and stiffness can directly affect the bandwidth and displacement output of the overall dual stage servo system. Finite element analysis (FEA) was employed to select the structural parameters and simulate its performance. Fig. 8 shows the FEA stress distribution. To simplify the analysis, we removed the center cross point and made the four ends of the spring beams constrained. It is observed that stress concentration occurs on the constrained ends of the spring beams and the narrow neck. This should be taken into account when selecting the cross-section of the spring beams.
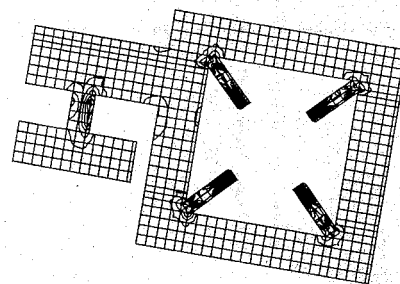
Fig. 8. FEM stress distribution of the cross-spring frame.

The first resonance mode of the cross-spring frame in the in-plane direction is illustrated in Fig. 9. The resonant frequency is about 10.9 kHz. It is also observed that the four spring beams are deformed to generate the desired angular displacement. To be a good design, The outside frame and the force arm should have no deformation. As expected, the narrow neck is also bent to protect the piezoelectric stack element.
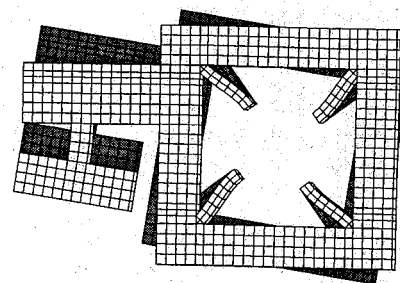
Fig. 9. First resonance mode of the cross-spring frame.

IV. EXPERIMENTAL RESULTS

Experiments were designed to measure the dynamic response of the piezoelectric stack micro-actuator with and without the HGA attached and with and without an air bearing. The experimental setup is shown in Fig. 10. A swept sine wave is generated through a HP Dynamic Signal Analyzer (DSA), amplified 20 times by a power amp., and

applied to the piezoelectric stack element. A Laser Doppler Vibrometer (LDV) is used to measure the in-plane motion. The laser beam is projected to the moving object and the motion of the measured object is then fed to the input channel of the DSA. The DSA compares the phase and magnitude of the original and feedback signals and generates a Bode Plot.

PIEZO AMPLIFIER: PIEZO SYSTEM. 60.102
LDV: VIBROMETER CONTROLLER POLYTEC OFV3001
FIBER INTERFEROMETER POLYTEC OFV502
DIGITAL SIGNAL ANALYZER: HP DSA 35670A
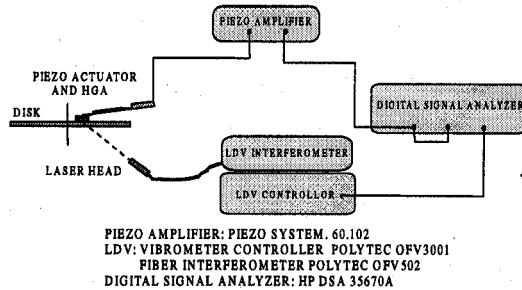
Fig. 10. Experiment setup for the piezoelectric micro-actuator.
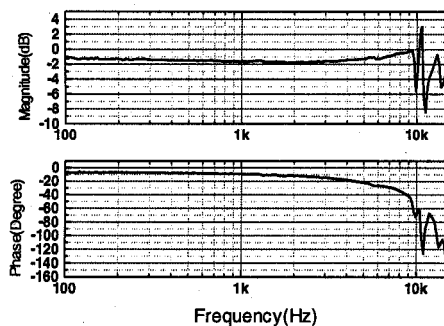
Fig. 11. Frequency response of the piezo-electric actuator without HGA.
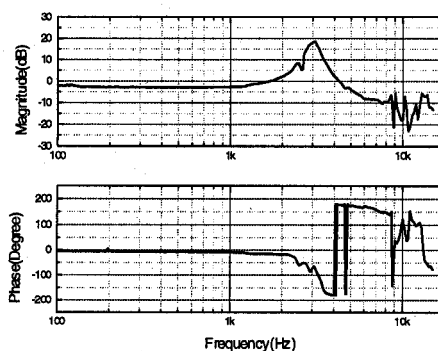
Fig. 12. Frequency response of secondary stage with HGA+air bearing.

Fig. 11. shows the frequency response of the piezoelectric micro-actuator without HGA attached to it. The measuring point is on the outside of the cross-spring frame. Its first resonance frequency is at about 10.6 kHz. However, the recording head is not mounted on the cross-spring frame, but on the tip of the HGA, i.e., the slider. The overall bandwidth of the secondary stage servo mechanism will be limited by the dynamics of both the loading beam and the gimbal. Fig 12 shows the frequency response of the secondary stage

mechanism + HGA measured when the slider is flying over the disk surface. The resonance peak is now shifted to 3 kHz. This is because of the existance of high stiffness air bearing.

In this design, the bandwidth of the overall secondary stage servo mechanism is limited by the bandwidth of the HGA's loading beam. To achieve the 25 kTPI target, high bandwidth HGA should be used. There are on going efforts to improve the bandwidth of the HGA [9,10].

V. DUAL STAGE SERVO CONTROL SCHEME

The structure and performance of the secondary actuator are key factors affecting the overall dual stage servo design. Generally, the ideal secondary actuator should possess the following properties: high bandwidth, sufficient displacement output, shock resistant capability, small size and simple structure, low cost, high reliability and long life cycle. The actuation should take place as close to the recording head as possible, but the electromagnetic field of the actuator should not affect the R/W process of the recording head.

Having looked at the design of the individual controllers for the two actuators, it was decided to design the dual actuator servo system such that the resultant transfer function has closed loop poles that are a product of the two individual servo loops. Fig. 13 shows the block diagram of the proposed dual actuator servo system. It includes a conventional VCM as the primary stage and the piezo micro-actuator as the secondary stage. It is assumed that there is no mechanical coupling between the two actuators which is a reasonable assumption considering the stiffness of the stacked piezo design.
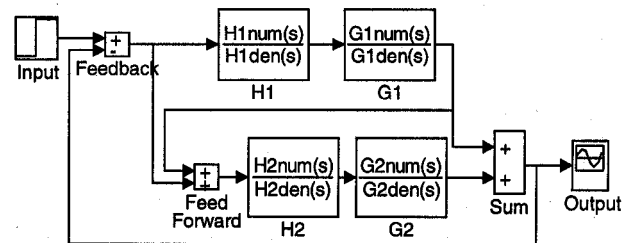
Fig. 13. Layout of the dual actuator servo system.

Let G_1 and G_2 be the plant for the VCM and the micro actuator. Let H_1 and H_2 be the controller for the VCM and the micro-actuator. Taking product of the denominators of the individual transfer functions $1+G_1H_1$ and $1+G_2H_2$ gives,

$$(1+G_1H_1)(1+G_2H_2) = 1 + G_1H_1 + G_2H_2 + G_1H_1G_2H_2 \quad (1)$$

The closed loop transfer function in fig. 13 takes the form,

$$\frac{G_1H_1 + G_2H_2 + G_1H_1G_2H_2}{1+G_1H_1 + G_2H_2 + G_1H_1G_2H_2} \quad (2)$$

Thus, the initial objective of combining and optimizing the two individual servo loop designs has been achieved. However, there is no guarantee that the resulting servo loop

will have good stability and performance. To tune the servo loop, the following performance guidelines were used,
1. High closed loop servo bandwidth.
2. To track low frequency disturbance by VCM
3. To track high frequency disturbance by micro-actuator.

These requirements were satisfied by shaping the micro-actuator servo loop to have a reduced low frequency gain and a increased high frequency gain through lead compensation. The lower servo bandwidth of the VCM will ensure that high frequency command or noise inputs will be tracked by the micro-actuator servo loop that is dominating with a higher gain. Fig. 14 shows the SIMULINK block diagram of the refined dual actuator controller design.
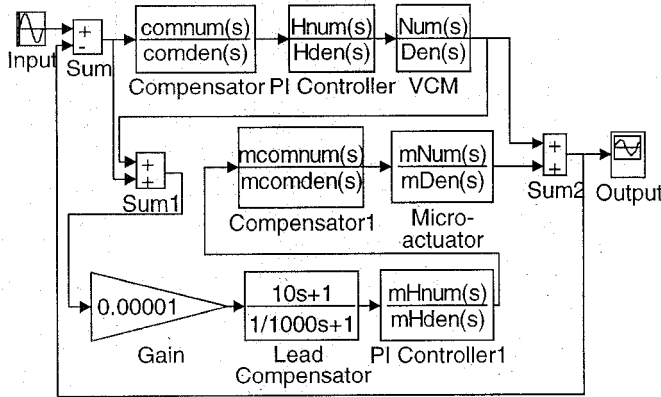
Fig. 14. SIMULINK block diagram of the dual actuator servo system.

Figures 15 and 16 show the bode plots of the individual servo loops. It can be seen that the micro-actuator servo loop has a higher gain at high frequencies. As a result, it dominates over the primary actuator. At low frequencies, it is the primary actuator or the VCM that is dominating over the micro-actuator.
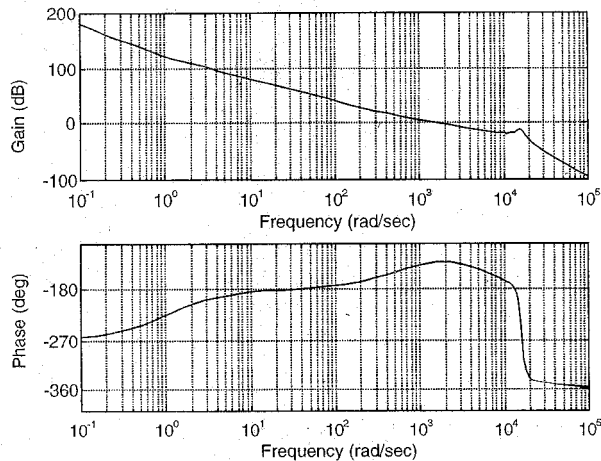
Fig. 15. Bode plot of VCM servo loop.

The dual actuator controller is also expected to have a higher servo bandwidth compared with using a single actuator. This can be seen in Fig. 17, which compares the closed loop bode plot of the dual actuator with that of just the

VCM. It is evident that the dual actuator has a much improved servo bandwidth.
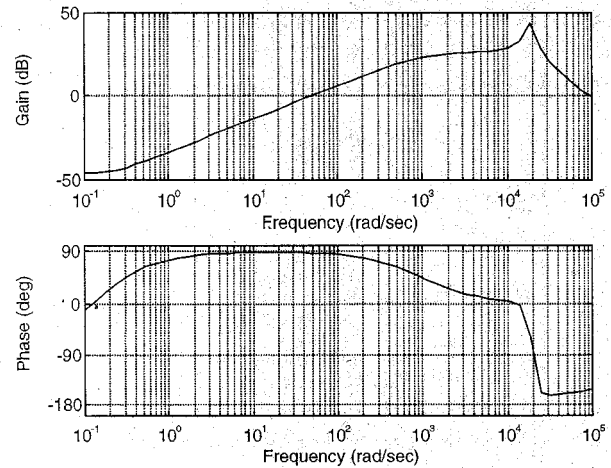
Fig. 16. Bode plot of the micro-actuator servo loop.
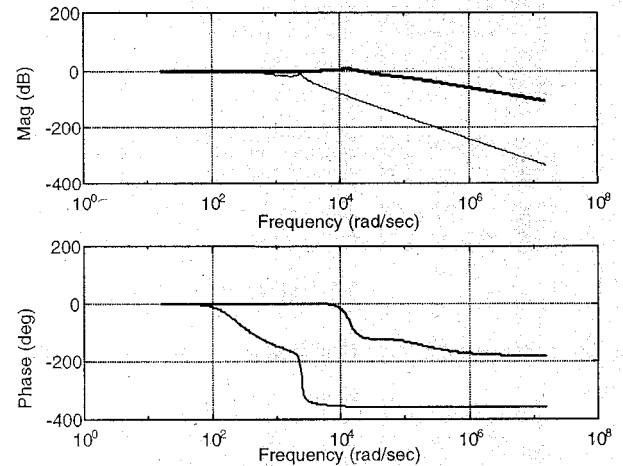
Fig. 17. Comparison of dual actuator controller with VCM controller.

From Fig. 14, it can be seen that dual actuator controller requires the VCM position to be fed into the micro-actuator controller. This is easy in theory but in practice, the VCM position is not available unless there is a relative motion detector at the interface between the primary and secondary actuators. One way to avoid such a costly sensor is to design a state estimator that will estimate the VCM position based on certain measurable inputs.

Assume that the only available measurement is the combined output of the dual actuator. The control commands to the two actuators are available from the servo controller. Therefore, it was decided to construct the estimator using the output track position, the input voltage to the micro-actuator and the current to the VCM.

The estimator is designed in state space as a predictive estimator. Four states x_1, x_2, x_3, and x_4, are defined where x_2 is the output of the micro-actuator, x_1 is $\dot{x}_2$, x_4 is the output of the VCM and x_3 is $\dot{x}_4$. The inputs u_1 and u_2

correspond to the micro-actuator and VCM respectively. The resonance mode of the VCM has been ignored in the design and the VCM is approximated as a second order transfer function. The estimator gain matrix L is calculated such that the resultant estimator poles would have faster dynamics than those of the controller. The SIMULINK block diagram of the resulting dual actuator controller is shown in Fig.18.
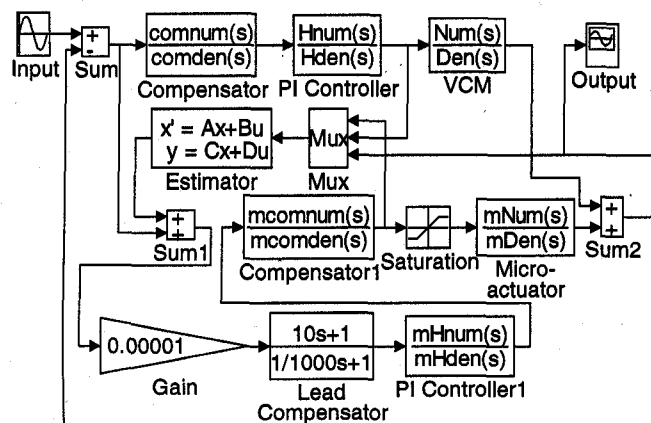
Fig. 18. Layout of dual actuator with state estimator.

The time domain simulation of a step response was done on the above model. The control command on the micro-actuator was saturated to 15 v to take into account the limited voltage magnitude available within the PC. The resulting time response is shown in Fig. 19. The effects of saturation on the dual actuator controller are minimal. Even for the step response, where the original input voltage is considerably above the saturation limit, the effect is hardly noticeable.
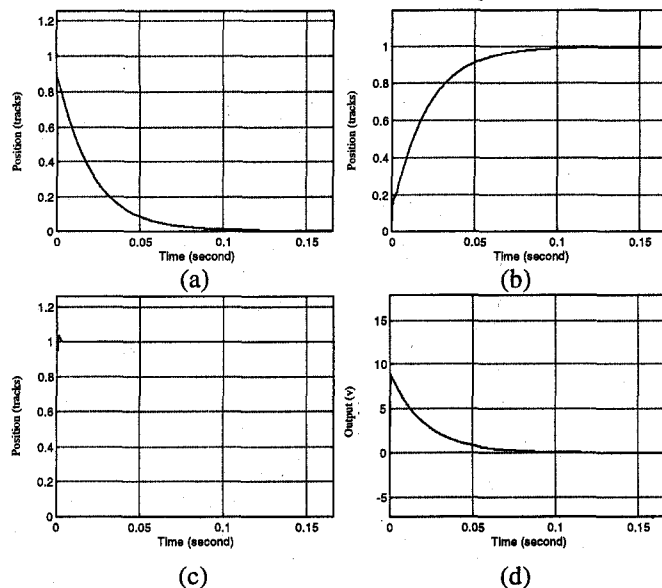
Fig. 19. One track seek performance of the dual actuator. (a) micr-actuator position (b) VCM actuator position (c) composite position (d) control input to micro-actuator

VI. CONCLUSIONS

Increase in bandwidth is constrained by the placement of the actuator resonance modes and other nonlinearities of the current VCM (voice coil motor) actuators. One approach to overcome this is by the use of a dual stage actuator, i.e. a VCM as a first stage and a smaller actuator as a secondary stage, to provide rapid small-motion and position correction of the recording head. Several dual-stage configurations have been proposed using electrostatic, piezoelectric and electromagnetic principles for the second stage. One piezoelectric stack micro-actuator with a cross-spring frame has been designed, fabricated, and tested. A servo system has been designed based on the measured plant model with a view to obtaining a higher bandwidth than with a single stage VCM. A bandwidth of 1.5 kHz has been demonstrated in simulations. The limited bandwidth is due to the relatively slower dynamics of the HGA. With a higher bandwidth HGA design, the dual actuator system may be able to achieve the performance required for track following at 25 kTPI track densities.

REFERENCES

[1] K.M. Tsuchiura, H.H. Tsukuba, H.O. Toride and T. Takahashi, "Disk System with Sub-actuators for Fine Head Displacement'. US Patent No. 5189578, Feb., 1993.

[2] D.K. Miu, "Silicon Micro-actuators for Rigid Disk Drives", Data Storage, pp 33-40, Jul./Aug., 1995.

[3] L.S. Fan, H.H. Ottesen, T.C. Reiley and R.W. Wood, "Magnetic Recording Head Positioning at Very High Track Densities Using a Microactuator-Based Two-Stage Servo System", IEEE Trans. on Ind. Elect., Vol.42, No.3, pp 222-233, Jun.,1995.

[4] K. Takaishi, T. Imamura, Y. Mizoshita, S. Hasegawa, T.Ueno and T. Ymada, "Micro-actuator Control for Disk Drive", IEEE Trans. on Mag., Vol. 32, No.3, pp 1863-1866, May, 1996.

[5] S. Koganezawa, K. Takaishi, Y. Mizoshita, Y. Uematsu, T. Yamada, S. Hasegawa and T. Ueno, "A Flexural Piggyback Milli-Actuator for Over 5Gbit/in.2 Density Magnetic Recording", IEEE Trans. on Mag., Vol.32, No.5, pp 3908-3910, Sept., 1996.

[6] K. Mori, T. Munemoto, H. Otsuki, Y. Ymaguchi and K. Akagi, "A Dual-Stage Manetic Disk Drive Actuator Using a Piezoelectric Device for a High Track Density", IEEE Trans. on Mag., Vol.27, No.6, pp 5298-5230, Nov., 1991.

[7] V. Temesvary, S. Wu, W.H. Hsieh, Y.C. Tai and D.K. Miu, "Design, Fabrication, and Testing of Silicon Microgimbals for Super-Compact Rigid Disk Drives", J. of Micro-electromechanical Sys.., Vol.4, No.1, pp18-27, pp 18-27, Mar., 1995.

[8] L.S. Fan, "Design and Fabrication of Micro-actuators for High Density Data Storage", IEEE Trans. on Mag., Vol.32, No.3, pp 1855-1862, May, 1996.

[9] "Technology Update: Seagate's 10K Drive Sets New Speed Mark", Data Storage, pp 8-12, Jan., 1997.

[10] D.K. Miu and R.M. Kara, "Dynamics and Design of Read/Write Head Suspensions for High Performance Rigid Disk Drives", Adv. Info. Storage Sys., pp 145-153, Vol.1, 1991.